Beating the Walker Limit with Massless Domain Walls in Cylindrical Nanowires

Ming Yan, Attila Kákay, Sebastian Gliga,[†] and Riccardo Hertel[*]

Institut für Festkörperforschung (IFF-9), Forschungszentrum Jülich GmbH, D-52428 Jülich, Germany

(Received 8 June 2009; published 1 February 2010)

We present a micromagnetic study on the current-induced domain-wall motion in cylindrical Permalloy nanowires with diameters below 50 nm. The transverse domain walls forming in such thin, round wires are found to differ significantly from those known from flat nanostrips. In particular, we show that these domain walls are zero-mass micromagnetic objects. As a consequence, they display outstanding dynamic properties, most importantly the absence of a breakdown velocity generally known as the Walker limit. Our simulation data are confirmed by an analytic model which provides a detailed physical understanding. We further predict that a particular effect of the current-induced dynamics of these domain walls could be exploited to measure the nonadiabatic spin-transfer torque coefficient.

DOI: 10.1103/PhysRevLett.104.057201 PACS numbers: 75.60.Ch, 75.40.Gb, 75.40.Mg, 85.75.−d

The controlled displacement of magnetic domain walls (DWs) along ferromagnetic nanostrips by means of electrical currents [1,2] has recently advanced to one of the most intensively studied topics in magnetism, both experimentally [3–9] and theoretically [10–16]. Much of this interest is aimed at the realization of a ''race track memory'' [3]—a promising concept for future magnetic data storage devices based on the current-driven DW displacement. In addition to this technological aspect, several complex nanomagnetic features make DW dynamics in thin strips attractive from a fundamental point of view. One example for this is the Walker breakdown [7,8,17–19], which occurs when DWs are driven strongly enough to reach a critical velocity of typically around a few 100 m/s. The DW structure then collapses and undergoes a series of complex cyclic transformations. This process is connected with a drastic reduction of the average DW speed. The Walker *limit* is thus the maximum velocity at which DWs can propagate in magnetic strips without changing their structure. For technological purposes such a limit represents a major obstacle, and various efforts have been made to overcome this limit [20,21].

In a broader physical context, the Walker limit is connected to the *mass* of the moving DWs. The concept of domain-wall mass was introduced in 1948 by Döring [22]. He discovered that the structure of a Bloch wall moving with velocity v differs from that of a static one, and that its energy increase is proportional to v^2. This allows one to formally define a kinetic energy and a mass. Moving DWs in thin magnetic strips in fact display particlelike behavior, including momentum and inertia [23]. Therefore the DW mass is not merely a mathematical abstraction: it gives rise to measurable effects, and, in particular, to the Walker limit. The connection between DW mass and Walker limit is given by the dynamic modification of the DW structure during its motion and the resulting increase of the energy density. The increase in energy continues until it reaches a limit where the micromagnetic structure collapses. Such a ''speed limit'' is therefore related to the kinetic energy and is inevitable for massive domain walls. The situation would be different if a DW did not change its structure during its motion. Such a DW would be massless and its kinetic energy would be zero, resulting in the absence of a Walker-type speed limit. In this Letter we show that such massless DWs indeed exist, namely, transverse walls in thin cylindrical soft-magnetic nanowires. Both, their magnetic structure and dynamic properties differ significantly from those of the well-known transverse DWs in thin strips. Contrary to their ''flat'' counterparts [24], we find that these DWs only change their position and orientation as they propagate, while their internal magnetic structure remains unchanged. The vanishing DW mass leads to astounding dynamic properties. Besides the absence of a critical velocity, we predict that the critical current required to initiate their motion is zero. Since high values of critical currents [3,10,11,13] also represent a major difficulty in applications, massless DWs in circular wires appear to be ideal candidates for devices based on DW propagation.

We investigate the dynamic properties of such DWs with micromagnetic simulations as well as analytically. The simulation studies are performed with our finite element algorithm which was extended [25] to consider also the current-induced magnetization dynamics as described by the Gilbert equation with additional spin-transfer torque terms [12,13]:

$$\frac{d\vec{M}}{dt} = \gamma \vec{H}_{\mathrm{eff}} \times \vec{M} + \frac{\alpha}{M_s}\left[\vec{M} \times \frac{d\vec{M}}{dt}\right] - (\vec{u}\cdot\vec{\nabla})\vec{M} + \frac{\beta}{M_s}\vec{M} \times [(\vec{u}\cdot\vec{\nabla})\vec{M}], \quad (1)$$

where $\vec{M}$ is the local magnetization, $M_s = |\vec{M}|$ the saturation magnetization, γ the gyromagnetic ratio, $\vec{H}_{\mathrm{eff}}$ the effective field, α the Gilbert damping factor, and β the nonadiabatic spin-transfer parameter [12,13]. The vector $\vec{u}$ is defined as

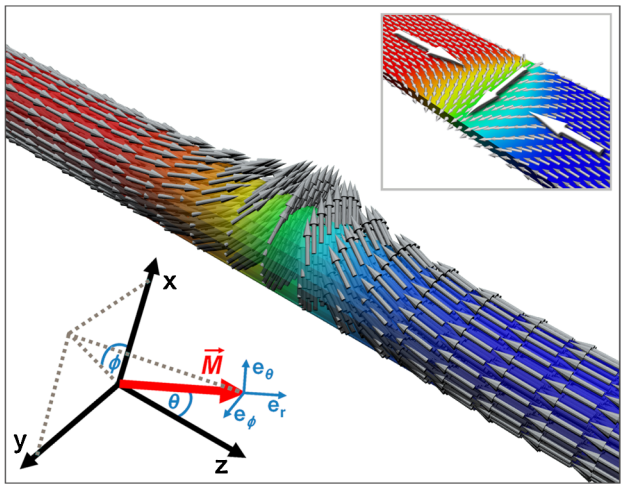

FIG. 1 (color online). A transverse DW formed in a 10 nm diameter cylindrical Py wire compared to a transverse wall in a 100 nm wide strip of 10 nm thickness (up-right). The Cartesian coordinate system and the spherical coordinate system used for the analytic study are shown on the lower left.

$$\vec{u} = -\frac{g\mu_B P}{2eM_s}\vec{j}, \tag{2}$$

where $\vec{j}$ is the current density, g is the Landé factor, μ_B the Bohr magneton, e the electron charge and P the polarization rate of the current. We consider Permalloy (Py) wires with material parameters $\mu_0 M_s = 1$ T, zero anisotropy, exchange constant $A = 1.3 \times 10^{-11}$ J/m, and $P = 0.7$. Figure 1 shows the simulated configuration of a transverse wall in a 4 μm cylindrical wire with 10 nm diameter. The wire volume is discretized into 259 200 tetrahedrons with cell size of about 1.25 nm $\times$ 1.25 nm $\times$ 5 nm. Because of the axial symmetry, the structure of the wall and its energy are invariant with respect to rotations of the magnetization in the xy plane.

An electrical current along $+z$ displaces the DW towards the $-z$ direction, i.e., in the electron flow direction. In addition to this linear motion the DW rotates about the axis of the wire, as illustrated schematically in Fig. 2. A similar type of spiralling DW motion in cylindrical wires has been reported for the field-driven case in Ref. [26]. The characteristics of this angular motion in the current-driven case will be discussed in more detail later. In the simulations, α is set to 0.02 while the value of β varies from 0 to 0.1. The DW velocity as a function of the current density j is shown in Fig. 3(a) for the case of a 10 nm diameter cylindrical wire and different values of β. The inset a_2 of Fig. 3 displays the lower range of current densities, as typically used in experiments. The results show that the velocity depends linearly on j and is independent of β. For comparison, we simulated the DW motion in a thin strip using the same parameters (inset a_1 of Fig. 3). The cylindrical wire displays several fundamental differences. First, there is no intrinsic pinning in the case when $\beta = 0$, while in the case of the strip a minimum (critical) current density

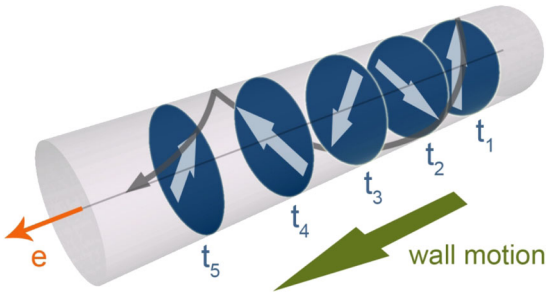

FIG. 2 (color online). Schematic illustration of the current-driven DW motion. The cross sections indicate the position of the wall plane at successive moments in time, while the arrows represent the orientation of the transverse magnetization. The gray spiral illustrates the precessional motion of the wall.

must be injected to drive the DW. Second, we observe that the DWs in the round wire behave like massless structures; i.e., their profile does not change during the motion [27]. Correspondingly, there is no Walker breakdown in the case of the cylindrical wire [28]. In the strip, however, a Walker limit occurs above a critical current density when $\beta > \alpha$,

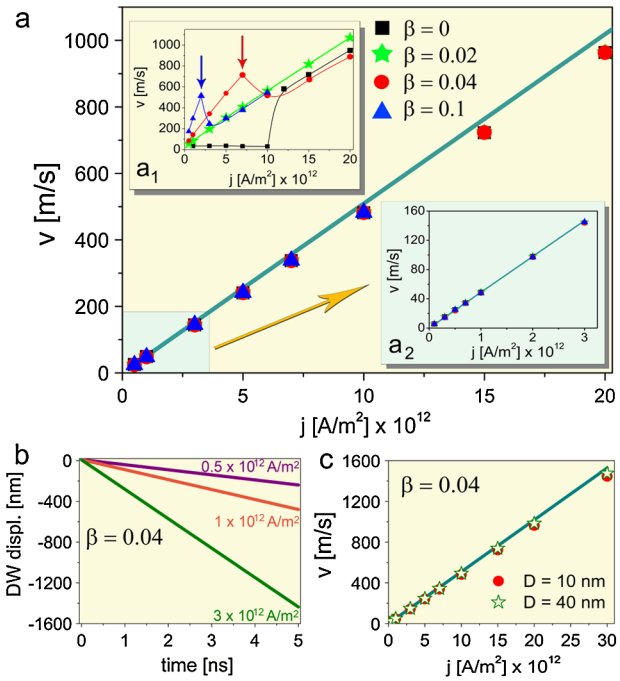

FIG. 3 (color online). (a) Simulated DW velocity as a function of the current density j for four different values of β in the case of a 10 nm round Py wire ($\alpha = 0.02$). Inset (a_1): Simulated DW dynamics in a 100 nm wide and 10 nm thick strip. (b) DW displacement as a function of time for three different values of j. (c) Comparison of the DW speed between the 10 and the 40 nm wire. The lines in (a), (a_2) and (c) are analytical values of u according to Eq. (2), while the lines in the inset (a_1) are guides to the eye. Excellent agreement with the analytic model is obtained, especially for lower values of the current density as shown in inset (a_2).

causing a significant drop of the propagation speed as indicated by the arrows in the inset a_1 of Fig. 3.

Third, the DW velocity does not depend on the value of β in the cylindrical wire, in striking contrast to the case of flat strips. In the round wire, the DW reaches a constant velocity immediately after the application of the current and stops at the moment the current is switched off. This behavior is consistent with the absence of mass and inertia of the wall. The resulting smooth DW motion is displayed in Fig. 3(b), which shows the DW displacement as a function of time for three values of j. A comparison of the DW speed in cylindrical thin wires of different diameters (10 and 40 nm) is shown in Fig. 3(c), indicating a very weak dependence on the wire thickness [29]. The characteristics of the angular dynamics are summarized in Fig. 4. Similar to the linear motion, the angular velocity shows a linear dependence on j. However, it also depends on β. More precisely, we find that this velocity is proportional to $(\beta - \alpha)$. The sense of rotation changes at $\alpha = \beta$, where the DW ideally does not rotate. Minor deviations from this ideal behavior observed in the simulations are due to finite-size effects [30].

To obtain a deeper physical understanding of the simulated data, we adopt an analytical model developed in Ref. [16]. A spherical coordinate system is used as shown in Fig. 1. The angular velocities of the magnetization can be related to the torques Γ acting on the wall [16]:

$$\dot{\theta} = \frac{d\theta}{dt} = -\frac{\gamma}{M_s}\Gamma_\theta, \tag{3a}$$

$$\dot{\phi} = \frac{d\phi}{dt} = -\frac{\gamma}{M_s}\Gamma_\phi. \tag{3b}$$

The expression for the total torque acting on the DW is given in Eq. 10 of Ref. [16], which takes into account a static magnetic field H applied along the z direction, the demagnetizing field, an equivalent damping field, and an electric current flowing in z direction. Using the cylindrical symmetry of the wire and considering only the center ($\theta = \pi/2$) of the DW like in Ref. [16], all terms pertaining to the demagnetizing field can be dropped. This leads to

$$\Gamma_\theta = \frac{\alpha M_s}{\gamma}\dot{\phi} + \frac{M_s u}{\gamma}\frac{\partial\theta}{\partial z}\bigg|_{wc}, \tag{4a}$$

$$\Gamma_\phi = -M_s H - \frac{\alpha M_s}{\gamma}\dot{\theta} - \frac{\beta M_s u}{\gamma}\frac{\partial\theta}{\partial z}\bigg|_{wc}, \tag{4b}$$

where the subscript wc denotes the DW center. Limiting the analysis to the DW center is justified *a posteriori* by our simulations, which show that the DW profile remains unchanged during the motion, thereby making it sufficient to describe only the position and the orientation of the DW. For simplicity, we first consider the field-driven motion with a static field applied along the z direction. From Eq. (4) with $u = 0$ and Eq. (3) one obtains

$$\dot{\theta} = -\alpha\dot{\phi} \quad \text{and} \quad \dot{\phi} = \frac{\gamma H}{1+\alpha^2}. \tag{5}$$

In a static magnetic field the DW hence precesses with the Larmor frequency and moves along the wire as a result of the damping. In terms of propagation velocity, the *field-driven* motion of these DWs is not attractive because of the small prefactor α. This is consistent with previous micromagnetic simulations of cylindrical Ni wires [26]. Let us now consider the current-driven case. Equation (4) with $H = 0$ combined with Eq. (3) yields

$$\dot{\theta} = -\frac{(1+\alpha\beta)u}{1+\alpha^2}\frac{\partial\theta}{\partial z}\bigg|_{wc}, \tag{6a}$$

$$\dot{\phi} = \frac{(\beta-\alpha)u}{1+\alpha^2}\frac{\partial\theta}{\partial z}\bigg|_{wc}. \tag{6b}$$

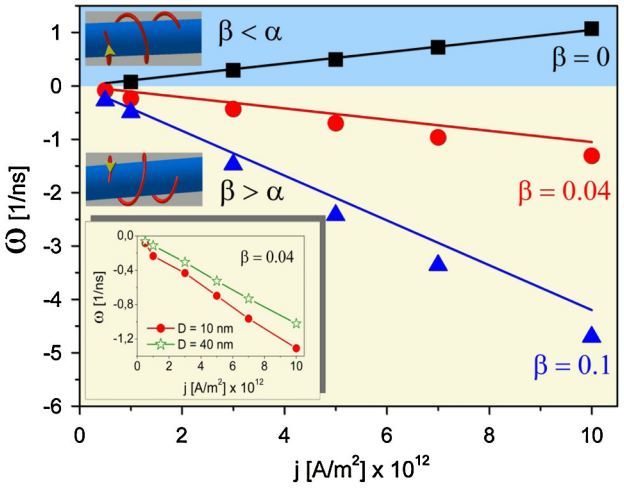

FIG. 4 (color online). Simulated angular DW velocity as a function of j for $\alpha = 0.02$ and three values of β in a round 10 nm Py wire. The lines represent analytic values (see text). Inset: Comparison between the angular DW velocity in the 10 and the 40 nm wire. The lines are guides to the eye.

These equations show how the adiabatic term influences the linear motion of the DW while the difference between the nonadiabatic parameter β and the damping coefficient α affects the rotational motion. In contrast to this, in the case of Bloch DWs or transverse DWs in strips, the damping and/or nonadiabatic terms lead to the distortion of the DW, i.e., to a nonvanishing mass and thereby to various undesirable effects such as the intrinsic pinning and the Walker limit. The critical current or field at the onset of the Walker breakdown is usually defined by the rotation of the central part of the DW out of the plane in which it originally lies, $\dot{\phi} \neq 0$ [13,16,17]. In our case however, given the symmetry of the wire, the DW is free to rotate without any deformation. The main features of our simulation results (summarized in Figs. 3 and 4) can be understood from Eqs. (6a) and (6b), which show that the linear velocity is independent of β and that the angular velocity depends on $(\beta - \alpha)$. This simple analytical model describes accurately the DW dynamics over a wide range of current densities. The predicted DW velocity is well reproduced

up to very large values of about 10^{13} A/m^2 [cf. Fig. 3(a)], above which minor deviations occur, indicating the onset of nonlinear dynamic effects. It is noteworthy that both $\dot{\theta}$ and $\dot{\phi}$ are proportional to $\partial\theta/\partial z|_{wc}$, which is related to the DW width. For the linear velocity, the DW width is not important, since $v = \dot{\theta}\partial z/\partial\theta$. The linear velocity is therefore basically equal to u [plotted as a line in Fig. 3(a)]. This explains why the linear speed is independent on the thickness of the wire as shown in Fig. 3(c), although the DW width is larger in the thicker wire. The angular velocity however shows a dependence on the DW width and therefore also on the wire thickness. This is consistent with the simulation results shown in the inset of Fig. 4, which show that the DW in the thicker wire has a lower angular velocity. The lines in Fig. 4 represent analytic values of the angular velocity for different β, obtained from Eq. (6b) by using a value of $\partial\theta/\partial z|_{wc}$ extracted from the simulated DW profile. According to this equation, the angular velocity should be identical if $(\beta - \alpha)$ has the same absolute value but opposite sign; a dependence that is almost perfectly confirmed by our simulations. A slight asymmetry observed in the simulations between $\pm(\beta - \alpha)$ is due to magnetostatic finite-size effects [30].

The dependence of the frequency of the DW rotation on the difference between α and β opens an interesting possibility for the measurement of the nonadiabatic spin-transfer torque parameter β, which is generally difficult to determine [31]. The characteristics of the field- and the current-induced DW dynamics in circular wires should allow for a precise extraction of this information. Firstly, according to Eq. (5), the value of α can be derived from the field-induced DW velocity. Then the value of β can be obtained from the frequency of the current-induced dipolar oscillations predicted by Eq. (6b) [32]. Also, the polarization rate P can be determined from the current-driven DW velocity, which in this case is almost exactly equal to u [cf. Figs. 3(a) and 3(c)].

In conclusion, the current-induced motion of transverse DWs in cylindrical nanowires is fundamentally different from that in magnetic strips. The DW velocity simply depends linearly on the current density j. Two important features usually limiting the dynamics of DWs, namely, the intrinsic pinning and the Walker limit, do not exist for this type of DW. This is attributed to a vanishing DW mass. Such inertia-free DWs show particular dynamic properties which should allow one to precisely and efficiently control their position with electric currents and to extract important physical parameters. The dynamics of these DWs thus deserves experimental investigation for both fundamental physical studies and applications.

*Corresponding author.
r.hertel@fz-juelich.de
†Present address: Center for Nanoscale Materials, Argonne National Laboratory, Argonne Illinois 60439 USA.

[1] L. Berger, Phys. Rev. B **33**, 1572 (1986).
[2] L. Berger, J. Appl. Phys. **63**, 1663 (1988).
[3] S. S. P. Parkin, M. Hayashi, and L. Thomas, Science **320**, 190 (2008).
[4] N. Vernier *et al.*, Europhys. Lett. **65**, 526 (2004).
[5] A. Yamaguchi *et al.*, Phys. Rev. Lett. **92**, 077205 (2004).
[6] E. Saitoh, H. Miyajima, T. Yamaoka, and G. Tatara, Nature (London) **432**, 203 (2004).
[7] M. Kläui *et al.*, Phys. Rev. Lett. **95**, 026601 (2005).
[8] M. Kläui *et al.*, Appl. Phys. Lett. **88**, 232507 (2006).
[9] M. Hayashi *et al.*, Phys. Rev. Lett. **98**, 037204 (2007).
[10] G. Tatara and H. Kohno, Phys. Rev. Lett. **92**, 086601 (2004).
[11] Z. Li and S. Zhang, Phys. Rev. Lett. **92**, 207203 (2004).
[12] S. Zhang and Z. Li, Phys. Rev. Lett. **93**, 127204 (2004).
[13] A. Thiaville, Y. Nakatani, J. Miltat, and Y. Suzuki, Europhys. Lett. **69**, 990 (2005).
[14] S. E. Barnes and S. Maekawa, Phys. Rev. Lett. **95**, 107204 (2005).
[15] S. M. Seo, W. J. Kim, T. D. Lee, and K. J. Lee, Phys. Status Solidi B **244**, 4460 (2007).
[16] A. Mougin *et al.*, Europhys. Lett. **78**, 57007 (2007).
[17] N. L. Schryer and L. R. Walker, J. Appl. Phys. **45**, 5406 (1974).
[18] M. Hayashi *et al.*, Nature Phys. **3**, 21 (2007).
[19] G. S. D. Beach *et al.*, Nature Mater. **4**, 741 (2005).
[20] Y.-S. Choi *et al.*, arXiv:0812.4083.
[21] E. R. Lewis *et al.*, Phys. Rev. Lett. **102**, 057209 (2009).
[22] W. Döring, Z. Naturforsch. **3**, 373 (1948).
[23] M. Kläui, J. Phys: Condens. Matt. **20**, 313001 (2008).
[24] R. D. McMichael and M. J. Donahue, IEEE Trans. Magn. **33**, 4167 (1997).
[25] Y. Liu, S. Gliga, R. Hertel, and C. M. Schneider, Appl. Phys. Lett. **91**, 112501 (2007).
[26] R. Hertel, J. Magn. Magn. Mater. **249**, 251 (2002).
[27] In our simulations we could not detect any DW mass, but we cannot conclude that the DW mass is exactly equal to zero. Whether the DWs are rigorously or practically massless is unimportant for the present study.
[28] The absence of the Walker limit does not imply that these DWs can move arbitrarily fast. Ultimately, a physical limit should occur when strong nonlinear effects develop during the motion. We could however not observe such a limit, since the DWs remain stable even when driven with unrealistically large currents above 10^{13} A/m^2, which exceeds the nucleation threshold. In this case the DW dissolves by propagating into newly nucleated domains.
[29] This behavior only holds as long as the wire is thin enough to form transverse walls. At wire diameters above about 50 nm vortex-type DWs with significantly different dynamic properties develop.
[30] Magnetic surface charges at the ends of our 4 μm long wire give rise to a small axial field that increases towards the ends of the wire. As the DW moves away from the central position, this magnetostatic field slightly but systematically affects the DW dynamics.
[31] S. Lepadatu *et al.*, Phys. Rev. B **79**, 094402 (2009).
[32] A detailed discussion on the measurement of β based on the combination of field- and current-induced DW dynamics will be given in a forthcoming paper.